ISSN: 2688-8645

Impact of Fracturing Fluid Fluid-Loss Characteristics on Oil Displacement Efficiency and Underlying Mechanisms

Zhi Li

School of Petroleum Engineering, Xi'an Shiyou University, Xi'an Shaanxi, 710000, China

Abstract

In previous studies, efforts regarding fracturing fluid fluid loss have predominantly aimed at "fluid loss reduction." This study, however, focuses on shifting from "fluid loss reduction" to "fluid loss promotion." This paper combines orthogonal experimental design with nuclear magnetic resonance (NMR) technology to reveal the mechanism by which fracturing fluid fluid loss distance affects displacement efficiency in unconventional reservoirs. Experiments found significant correlations between fluid loss distance and injection pressure differential, reservoir permeability, and fracture morphology parameters. Among these, permeability has the highest influence factor at 62.3%, making it the key factor affecting seepage distribution. Three different types of fracturing fluids were selected for this study—LGF-80 fracturing fluid, CNI fracturing fluid, and bio-based nano-oil-displacement fracturing fluid—to conduct research from a multi-factor, multi-level perspective, exploring the optimal conditions for each factor. The bio-based fracturing fluid system developed based on nanotechnology demonstrates significant advantages over traditional LGF-80 and CNI systems, achieving markedly improved displacement efficiency in low-permeability core experiments. The dynamic imbibition-NMR coupling measurement method proposed in this work overcomes the limitations of traditional fluid loss volume evaluation and provides important reference value for improving field displacement efficiency.

Keywords

Fracturing Fluid; Filtration Loss; NMR.

1. Introduction

According to the latest data from the China Petroleum and Chemical Industry Federation, China's external dependence on oil and gas reached 72% and 41% respectively in the first quarter of 2024[1]. The severity of the energy security situation underscores the strategic value of enhanced oil recovery (EOR) technologies. In the field of unconventional oil and gas development, volumetric fracturing technology has become the core method for the economical development of tight oil/shale oil and gas[2-5]. However, the design of traditional fracturing fluid systems universally faces a process contradiction between "fracture creation capability" and "imbibition displacement": high-viscosity, low-fluid-loss systems can form complex fracture networks[6] but limit the effective imbibition of fracturing fluid into matrix micro-nano pores; while enhancing fluid loss can increase matrix sweep volume[7], it may lead to a reduction in fracture conductivity. Current research primarily focuses on controlling fracturing fluid loss volume[8-12], and there remains a lack of systematic understanding of the dynamic correlation mechanism between the key parameter of fluid loss distance and displacement efficiency.

ISSN: 2688-8645

2. Physical Simulation Experiments and Methods

2.1. Materials

Three fracturing fluid systems were used in the experiments:

1. **LGF-80 Solution:**

Formula 1: Mixing water + 0.27% XYZC-6 + 0.6% XYTJ-3

Formula 2: Mixing water + 0.50% XYZC-6 + 0.6% XYTJ-3

2. CNI Fracturing Fluid:

Formula 1: Fresh water + 0.08% CNI-B + 0.08% CNI-A + 0.03% CQ-Z01

Formula 2: Fresh water + 0.20% CNI-B + 0.08% CNI-A

Formula 3: Fresh water + 0.30% CNI-B + 0.08% CNI-A

3. Bio-based Nano-Oil-Displacement Agent.

Experimental materials included quartz sand-epoxy resin artificial cores with three different permeabilities (50 mD, 100 mD, 150 mD) (approximately 2.5 cm in diameter, 2.5 cm in length). Subsequently, these artificial cores were sheared to create fractures, and plastic spacers were inserted as shown in Figure 1. Da Dong Gou crude oil with a density of 0.675 kg/m^3 and simulated formation water were also used.

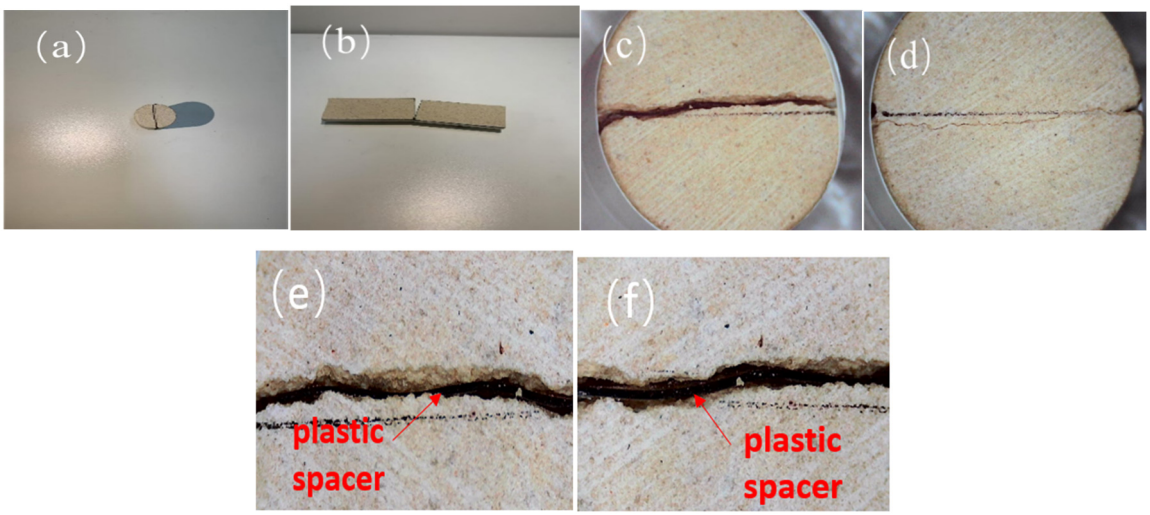

Figure 1. Quartz Sand-Epoxy Resin Artificial Cores

2.2. Fluid Loss Distance Evaluation Experimental Setup

For calculating fluid loss distance, and considering the need to determine oil saturation, vacuum saturation with oil was chosen. This method utilizes vacuum pumping to remove gas from the pores of the core or other porous media, allowing oil to fully fill these pores. Pressure is increased during the saturation process to ensure the core is fully saturated with oil. Under vacuum conditions, gas pressure decreases, affecting its presence in the pores. As the saturation vapor pressure of oil is much lower than that of water and gas, after gas is expelled under specific vacuum conditions, oil can readily enter and occupy the pore space. Subsequently, combined with NMR technology, the change in oil saturation before and after core displacement is calculated by comparing the area changes under the T_2 relaxation spectrum curves before and after.

Main experimental equipment included an ultra-low permeability core vacuum pressure saturation apparatus and a high-temperature, high-pressure dynamic imbibition-displacement experimental device (comprising a constant flow pump, temperature control system, pressure

ISSN: 2688-8645

application device, imbibition cell, intermediate containers, pressure sensors, and liquid collection devices).

Considering that fracturing fluid type, fluid loss time, injection pressure differential, and permeability all impact fluid loss distance during actual fracturing, and that fluid loss volume gradually increases as the fracture extends, a fluid loss distance evaluation experiment was designed. The experimental setup is shown in Figure 3. Five quartz sand-epoxy resin artificial core segments were combined to simulate an artificial fracture. During the experiment, the length of plastic spacers within the core segments was adjusted to simulate fracture propagation and the fracturing fluid fluid loss process.

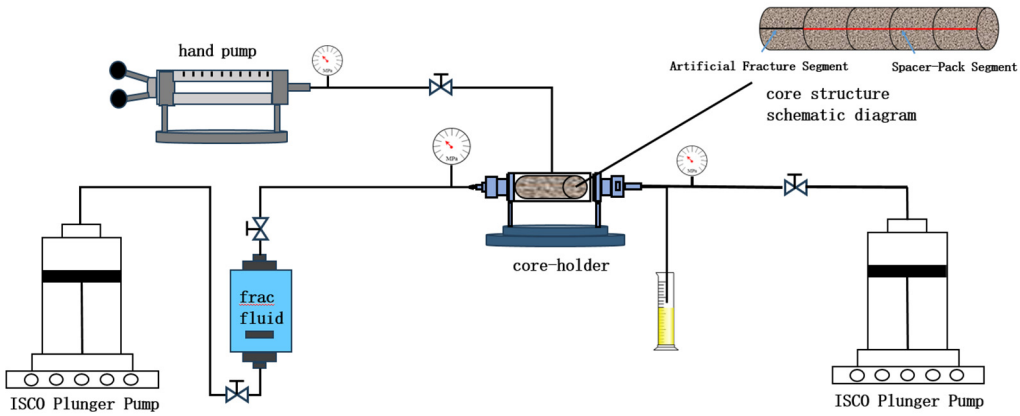

Figure 2. Dynamic Imbibition-Displacement Process

2.3. Fluid Loss Distance Evaluation Method

Considering conditions of high fracturing fluid viscosity and homogeneous cores, the movement of fracturing fluid within the porous medium is approximated as piston-like displacement. The fluid loss distance is calculated as:

$$L = \frac{V}{A\,\phi(Soi - Sor)} \quad (1)$$

Where:

L = Fluid loss distance, cm,**V** = Fluid loss volume, ml

A = Core cross-sectional area, cm^2

ϕ = Porosity, %

S_{oi}= Initial oil saturation

S_{or} = Residual oil saturation after fracturing fluid displacement

The specific evaluation method is as follows:

1. Five core segments were sheared transversely using a vise to create fractures. This method helps create fractures as close as possible to natural fractures. The cores were weighed, vacuum-saturated with water, weighed wet, and pore volume was calculated.

2. The core segments were assembled together with plastic spacers of equal length placed between them. The assembly was wrapped with PTFE (Teflon) tape to form a series connection of the five segments. This assembly was placed in a core holder and saturated with oil to calculate initial oil saturation.

3. The core assembly was removed, the PTFE tape and internal spacers were removed. Plastic spacers were re-inserted according to the required penetration ratio. The assembly was rewrapped with tape and placed back into the core holder. Fracturing fluid was injected at

ISSN: 2688-8645

pressure differentials of 2 MPa, 5 MPa, and 10 MPa. Effluent was collected to calculate fluid loss volume.

4. The calculated fluid loss volume was substituted into formula (1) to derive the fluid loss distance.

5. By comparing fluid loss distances under different parameter conditions, the optimal conditions for fracturing fluid fluid loss effectiveness were determined.

2.4. Oil Displacement Efficiency Calculation Method

The experiment combined NMR curves to calculate displacement efficiency. When scanning NMR curves, since the fracturing fluid contains water and the core contains irreducible water, research indicated that manganese-doped water ($MnCl_2$ solution) could be used to suppress the water signal. Adding a 20% concentration of Mn-doped water achieved 99.99% suppression of the water signal. Thus, the NMR curve results only reflected the oil saturation within the core, allowing displacement efficiency to be calculated based on changes in the NMR curve area. After initial core saturation with oil, the oil saturation was considered 100%, and the area under the NMR curve at this point was calculated. After the displacement experiment, the core was scanned again with NMR, and the area under the curve was recalculated. The change in area values yielded the displacement efficiency for that stage. Repeating this process determined the change in displacement efficiency for each core segment.

3. Experimental Results

3.1. Study on Fluid Loss and Displacement Efficiency in High-Permeability Sandstone under Different Parameters

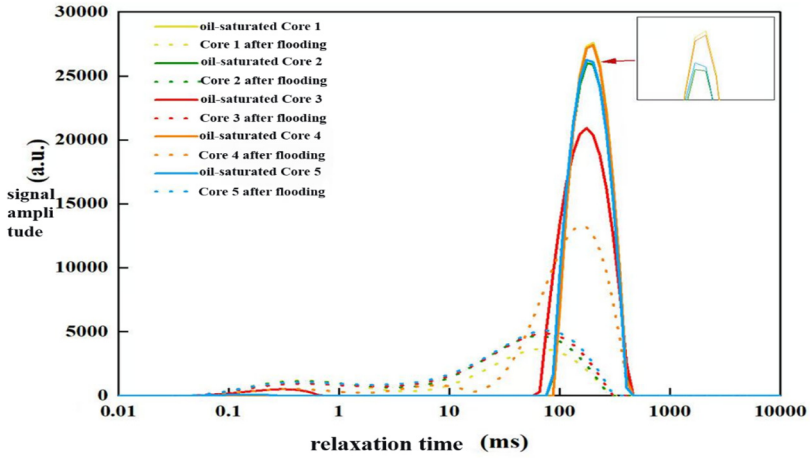

Figure 3. NMR Scan Results for Five Core Segments under 2 MPa, 2.5 cm, 50 mD Conditions

The orthogonal experimental method was employed to simultaneously consider the influence of multiple factors on the experimental results and determine the interactions between factors and the optimal factor combination. Experiments were first conducted using LGF-80 fracturing fluid. Oil saturation was calculated using NMR technology by comparing the area changes under T_2 relaxation spectra before and after displacement, as shown in Figure 3. Figure 3 shows the T_2 spectrum area change before and after displacement under conditions of 2 MPa injection pressure differential, 2.5 cm fracture size, and 50 mD permeability. In the figure, the solid curve represents the NMR curve after oil saturation, while the dashed curve represents the NMR curve after displacement. The oil saturation change obtained by this method is precise. After obtaining the oil saturation value, the relevant values were substituted into formula (1) to derive the fluid loss distance, shown in Table 1. Table 1 shows that the maximum calculated

ISSN: 2688-8645

fluid loss distance occurred under conditions of 10 MPa injection pressure differential, 100 mD permeability, and 5 cm fracture size. This indicates that among the nine different factor-level combinations in Table 1, this combination yielded the best results. Furthermore, using the orthogonal experimental method, range analysis performed with SPSSAU software allowed for the optimization of the best parameter combination.

Table 1. Specific Data from Fluid Loss Distance Evaluation Experiments

Injection Pressure Differential (MPa)	Permeability (mD)	Fracture Size (cm)	Residual Oil Saturation	Fluid Loss Distance (cm)
2	50	2.5	0.77363003	0.024
5	100	2.5	0.479437	0.2115
10	150	2.5	0.544568	0.1864
10	100	5	0.513145	0.2398
5	50	5	0.842242975	0.034
2	150	5	0.913768	0.012
2	100	7.5	0.525504	0.228
5	150	7.5	0.898637	0.0176
10	50	7.5	0.709473	0.0489

3.1.1. Influence of Injection Pressure Differential

After calculating fluid loss distance using formula (1), the data for different factors and levels along with their corresponding fluid loss distances were input into SPSSAU software for dynamic analysis. The relationship between injection pressure differential and fluid loss distance is shown in Figure 4. Figure 4 indicates that under pressure differentials from 2 MPa to 5 MPa, the mean value remained relatively stable without significant growth. This suggests that displacement effectiveness was poor and stable under differentials of 2-5 MPa, likely due to the insufficient pressure differential for effective displacement of crude oil from core pores by the fracturing fluid. When the pressure differential exceeded 5 MPa, the mean value began to increase steadily. At this point, as the pressure differential increased, experimental effectiveness improved progressively until reaching 10 MPa. This is attributed to efficient displacement of oil from core pores starting at a differential of approximately 5 MPa. Therefore, the relationship between pressure differential and fluid loss distance is: below 5 MPa, the differential has an insignificant effect; above 5 MPa, it is directly proportional and its influence becomes increasingly significant.

3.1.2. Influence of Fracture Size

Three different levels of fracture size (2.5 cm, 5 cm, 7.5 cm) were selected and combined with other factors. The method for analyzing the relationship between fracture size and fluid loss distance was the same as that used for pressure differential. The data was imported into SPSSAU software for dynamic analysis. Figure 4 shows that as fracture size increased,

ISSN: 2688-8645

experimental effectiveness deteriorated rapidly until the size reached 5 cm. This is attributed to the insertion of plastic spacers, which caused the fracturing fluid to split and flow along both sides of the spacer. Compared to having no spacer, this increased the swept volume of fracturing fluid through the core pores, thereby enhancing displacement efficiency and improving experimental results. Within this size range, fluid loss distance was inversely proportional to fracture size. When fracture size reached 5 cm, further increases resulted in only marginal improvement, with results stabilizing.

3.1.3. Influence of Permeability

Artificial cores with different permeabilities (K=50 mD, 100 mD, 150 mD) were used, each orthogonally combined with various levels of the other factors. The resulting data was imported into SPSSAU software for dynamic analysis. Figure 4 shows that among the three permeabilities, 100 mD yielded the best experimental results, followed by 150 mD, with 50 mD performing the worst. The influence of permeability on fluid loss distance exhibited an initial increase followed by a decrease. As permeability increased from 50 mD to 100 mD, it is considered that the inaccessible pore volume for fracturing fluid within the core decreased, increasing the swept volume. Consequently, displacement efficiency increased, and fluid loss distance was directly proportional to permeability. When permeability exceeded 100 mD, its positive influence gradually diminished.

3.1.4. Comparative Analysis of Different Factors

By analyzing the factors of injection pressure differential, fracture size, and permeability, and comparing them, the conditions for optimal displacement efficiency were determined: injection pressure differential of 10 MPa, fracture size of 2.5 cm, and permeability of 100 mD. Under these conditions, the displacement efficiency of the fracturing fluid reached its optimum state, consistent with the range analysis results. This leads to the summary shown in Figure 4.

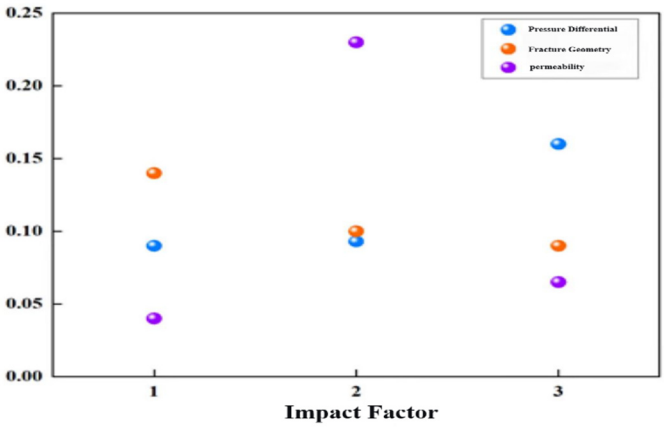

Figure 4. Mean Plots for Each Factor Level

3.2. Comparison of Fluid Loss and Displacement Efficiency for Different Fracturing Fluid Types in Low-Permeability Reservoirs

3.2.1. CNI Fracturing Fluid Fluid Loss Effectiveness Evaluation

To analyze the influence of fracturing fluid type on fluid loss distance, all variables except the fracturing fluid were controlled under identical conditions: injection pressure differential of 2 MPa, permeability of 50 mD, fracture size of 5 cm. The experimental results are as follows:

Figure 5 shows the NMR scan results before and after displacement using CNI fracturing fluid under the conditions of 2 MPa injection pressure differential, 50 mD permeability, and 5 cm fracture size. The solid curve represents the NMR scan after oil saturation, and the dashed curve represents the NMR scan after displacement.

ISSN: 2688-8645

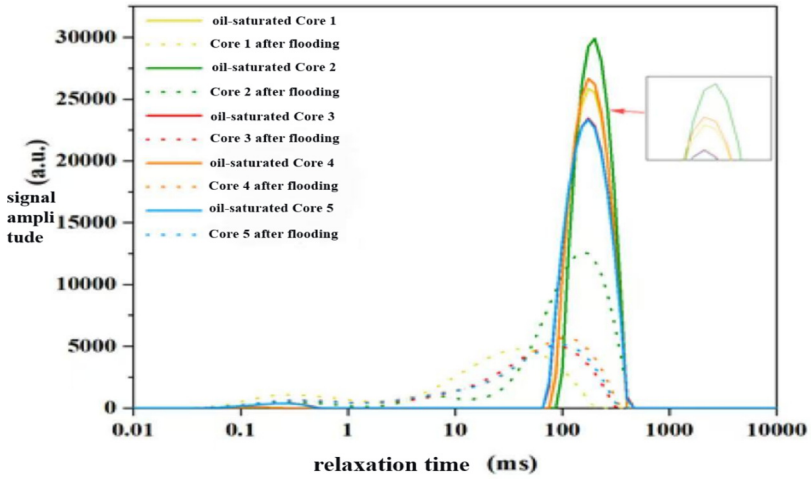

Figure 5. NMR Scan Results Before and After Displacement for Samples 1-5 (CNI fluid, 2 MPa, 50 mD, 5 cm)

The change in oil saturation before and after displacement can be derived from the difference in the area under the curves. The NMR area changes for samples 1~5 are highly significant, indicating that a large amount of oil was displaced from the cores. Furthermore, the relaxation time before displacement ranged between 65~464 ms; the starting point of the relaxation time reflects pore size. After displacement, the relaxation times of the cores changed, with the starting points shifting leftwards, indicating a reduction in pore volume within the cores after displacement.

3.2.2. Bio-based Nano-Oil-Displacement Fracturing Fluid Fluid Loss Effectiveness Evaluation

Figure 6 shows the NMR scan results before and after displacement using the bio-based nano-oil-displacement fracturing fluid under the conditions of 2 MPa injection pressure differential, 50 mD permeability, and 5 cm fracture size. The solid curve represents the NMR scan after oil saturation, and the dashed curve represents the NMR scan after displacement.

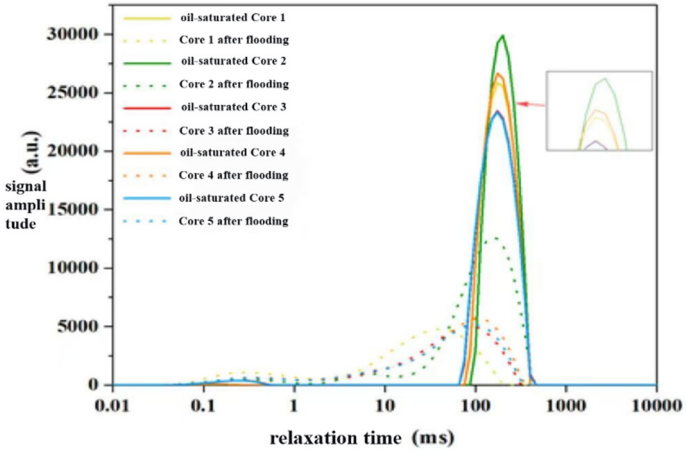

Figure 6. NMR Scan Results Before and After Displacement for Samples 1-5 (Bio-based Nano fluid, 2 MPa, 50 mD, 5 cm)

The change in oil saturation before and after displacement can be derived from the difference in the area under the curves. The NMR area changes for samples 1~5 are highly significant, indicating that a large amount of oil was displaced from the cores. Furthermore, the relaxation time before displacement ranged between 75~464 ms; the starting point of the relaxation time

ISSN: 2688-8645

reflects pore size. After displacement, the relaxation times of the cores changed, with the starting points shifting leftwards, indicating a reduction in pore volume within the cores after displacement.

3.2.3. Comparative Analysis of Different Fracturing Fluids

Combining the LGF-80 fracturing fluid experimental data with the CNI and bio-based nano-oil-displacement fracturing fluid data, a comparative analysis determined which fracturing fluid performed best under the same environmental conditions, as shown in Figure 7:

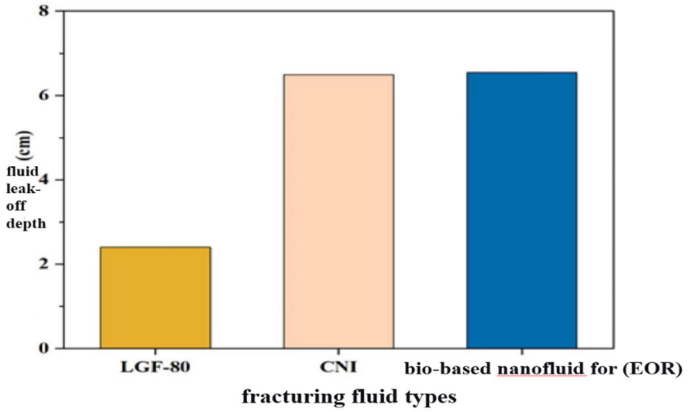

Figure 7. Comparison of Fluid Loss Distance Results for Three Different Fracturing Fluids

Figure 7 shows that under identical experimental conditions, among the different fracturing fluids, the bio-based nano-oil-displacement fracturing fluid achieved the best fluid loss effectiveness. The CNI fracturing fluid's effectiveness was close to but slightly inferior to the bio-based fluid. The LGF-80 fracturing fluid yielded the poorest fluid loss results.

4. Conclusion

The NMR-based dynamic characterization method for fluid loss distance provides a high-precision technical means for evaluating fracturing fluid performance. By adjusting factors influencing fracturing fluid behavior—such as core fracture size, permeability, and injection pressure differential—and selecting different types of fracturing fluids, the fluid loss effectiveness can be optimized, leading to improved oil displacement efficiency. Compared to fracture size and injection pressure differential, permeability has a significantly higher impact on fluid loss distance. Compared to LGF-80 and CNI fracturing fluids, the bio-based nano-oil-displacement fracturing fluid demonstrates the best fluid loss effectiveness and optimal displacement efficiency. Furthermore, through interfacial modification and rheological regulation, the bio-based nano fluid achieves high displacement efficiency in low-permeability cores, demonstrating significant potential for engineering application.

References

[1] Chen Yu. Why is the granting of oil and gas exploration rights accelerating [J]. Chinese oil companies, 2024, (07):51.

[2] Sun Xiang. Study on the Effect of Fracturing Fluid Filtration Characteristics on Oil Enhancement and Water Reduction [D]. Northeast Petroleum University,2018.

[3] Li Yang, Zhao Qingmin, Yang Yong, et al. Study and Practice on CO_2 Pre-Pad Fracturing Technology for Continental Shale Oil in Shengli Oilfield [J]. Fault-Block Oil and Gas Field, 2024, 31(06):945-954.

[4] Luo Di, Li Li, Ma Fengyuan, et al. Fracturing Practice and Insights in an Offshore Low-Permeability Oilfield Based on Geology-Engineering Integration: A Case Study from the Lufeng Sag, Pearl River Mouth Basin [J]. China Petroleum Exploration,2024,29(03):104-117.

[5] Wang Xiaobing, Hu Yanshe, Li Sen, et al. A Study on Fracture Conductivity and Productivity Models for Hydraulic Fracturing in Sedimentary Tight Oil Reservoirs [J]. Xinjiang Petroleum Geology,2023, 44 (04): 442-449.

[6] Huang Yi, Chen Haodong, Zheng Haopeng, et al. Study on the Influence of Casing Eccentricity on the Mechanical Integrity of the Cement Sheath in Fractured Wells [J]. China Offshore Oil and Gas,2022, 34 (06):135-141.

[7] Wu Qi, Xu Yun, Liu Yuzhang, et al. Current Status of Volumetric Stimulation Technology for Shale Gas in the United States and Its Implications for China [J]. Oil Drilling & Production Technology, 2011, 33(02):1-7.DOI:10.13639/j.odpt.2011.02.001.

[8] Lu Xiangguo, Cao Bao, Xie Kun, et al. A Well Fracturing Method Based on the Oil Displacement Effect During Fracturing Fluid Leak-off and Its Practical Results [J]. Oilfield Chemistry,2020,37(04):635-641. DOI:10.19346/j.cnki.1000-4092.2020.04.012.

[9] Pan He, Lu Xiangguo, Xie Kun, et al. Influence and Mechanism of Fracturing Fluid Filtration Characteristics on Oil Enhancement Effectiveness [J]. Oilfield Chemistry,2017,34(02):245-249. DOI: 10. 19346/j.cnki.1000-4092.2017.02.011.

[10] Hao Zhenxing. Analysis of Oilfield Fracturing Technologies and Optimization of Fracturing Fluids[J]. Chemical Engineering & Equipment.,2023,(03):38-39.DOI:10.19566/j.cnki.cn35-1285/tq. 2023. 03. 078.

[11] Cao Jianxun. Optimization and Selection of Oilfield Fracturing Technology and Fracturing Fluid[J]. Chemical Engineering & Equipment,2022,(05):59-60.DOI:10.19566/j.cnki.cn35-1285/tq. 2022. 05. 015.

[12] COOK C E. Effect of fracturing fluids on fracture conductivity[J]. J Pel Technol, 1975, 27(10): 1273-1282.